Electronic Supplementary Material (ESI) for Nanoscale.

Supporting Information

Ultrasound-controllable ROS-responsive nanoplatform for O_2 and NO generation to enhance sonodynamic therapy against multidrug-resistant bacterial infection

Jingyi Zhang[a,#], Lin Zhang[b,#], Yuhan Zhang[a], Rong Ju[a] and Guoqing Wei[a,*]

[a] *Chengdu Women's and Children's Central Hospital, School of Medicine, University of Electronic Science and Technology of China, Chengdu, 611731, PR China.*

[b] *Department of Neonatology, People's Hospital of Jianyang City, Jianyang, 641400, PR China.*

[#]*These authors contributed equally to this work.*

Corresponding author: E-mail: guoqing@uestc.edu.cn (G. Wei)

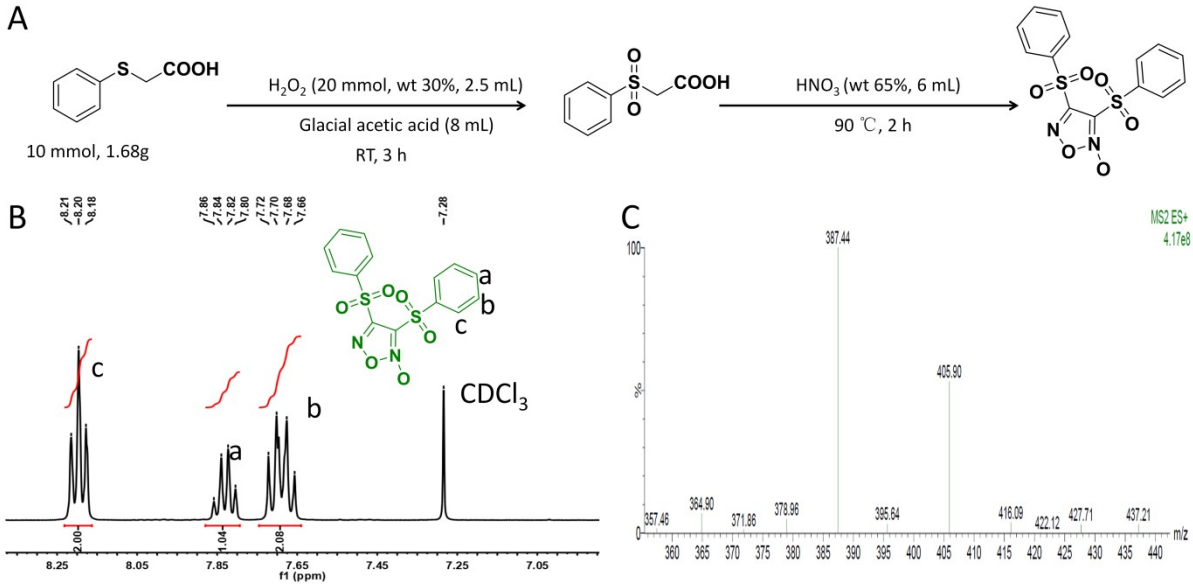

Figure S1. (A) Synthetic route and chemical structure of FOT. (B) ^{1}H NMR spectrum of synthesized FOT in $CDCl_3$ δ 8.20 (t, J = 4.0 Hz, 2H), 7.83 (dd, J = 16.0, 8.0 Hz, 1H), 7.66 (q, J = 8.0 Hz, 2H). (C) The MS of synthesized FOT.

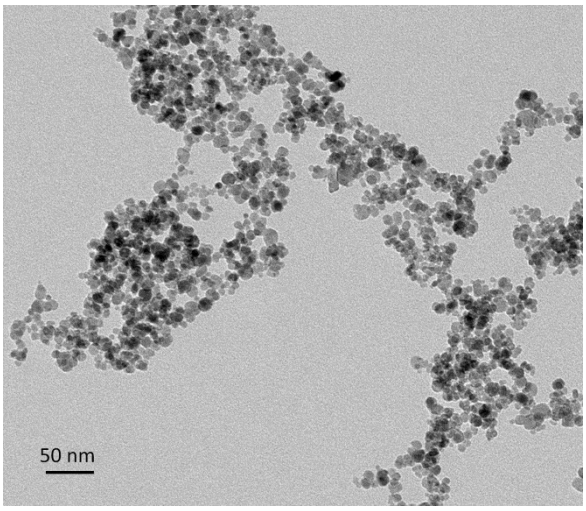

Figure S2. Transmission electron microscope images of Fe_3O_4 NPs.

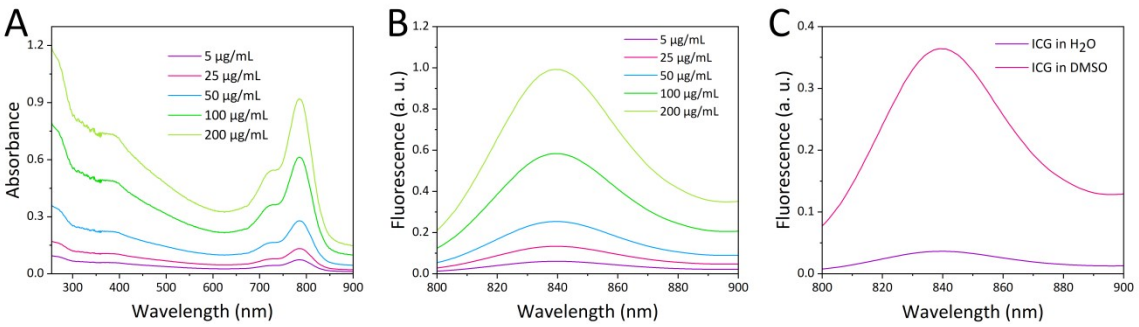

Figure S3. (A) UV−vis absorption spectra and (B) Fluorescence intensity of FOT/Fe_3O_4@Lipo-ICG at different concentration. (C) Fluorescence intensity of ICG in H_2O and DMSO.

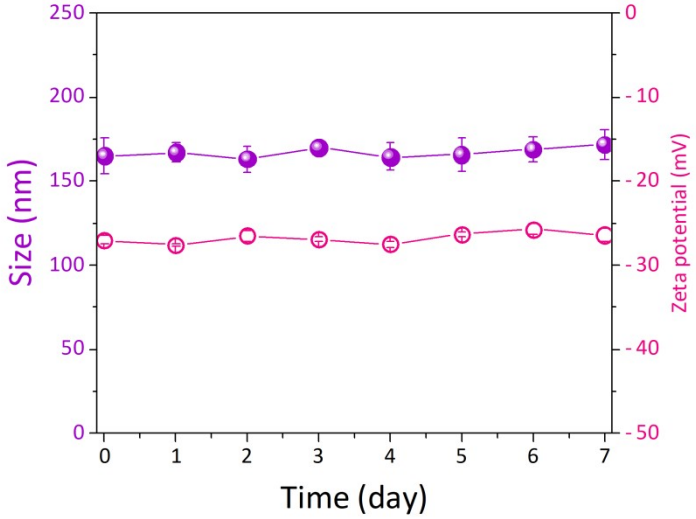

Figure S4. Colloidal stability of FOT/Fe_3O_4@Lipo-ICG in PBS. Data are presented as mean ± s.d. (n = 3).

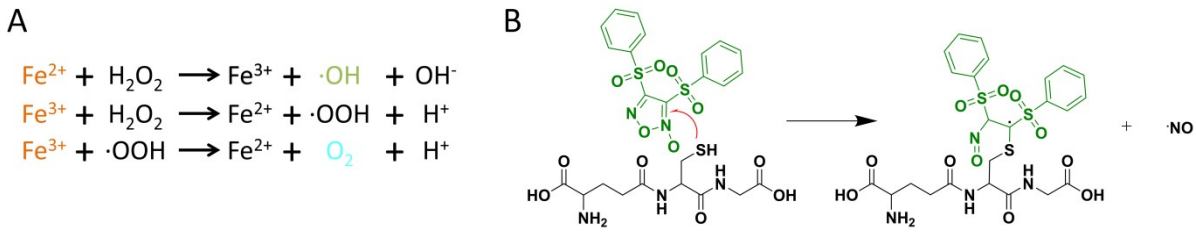

Figure S5. (A) The equations of the Fenton reaction. (B) The mechanism of GSH-mediated NO release from FOT.

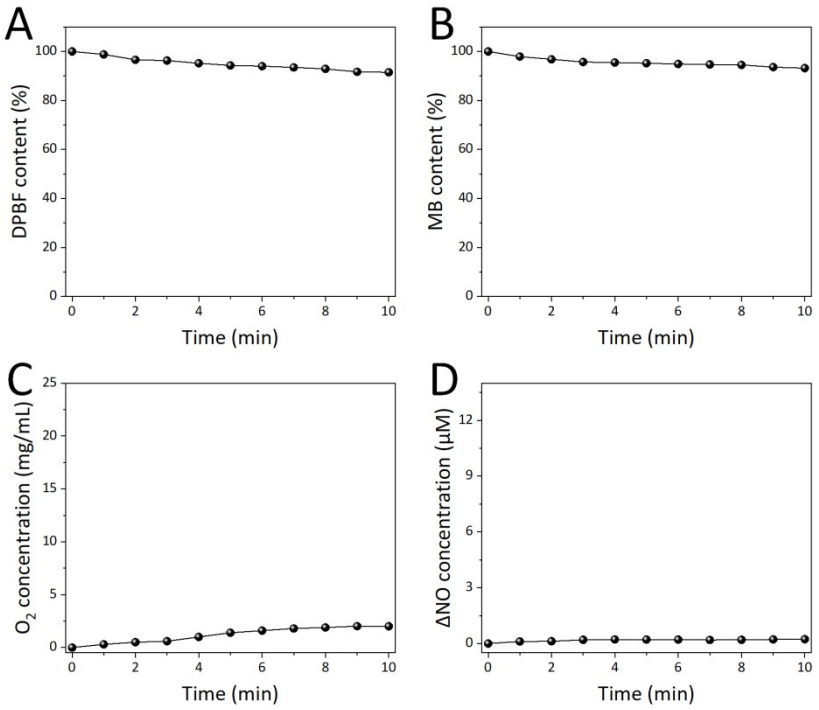

Figure S6. (A) Consumption of DPBF due to $\bullet O^{2-}$, (B) Consumption of MB due to •OH, (C) O_2 generation and (D) NO generation of H_2O_2 with US irradiation. US irradiation: 1.0 MHz, 1.0 W/cm2, 40% cycle.

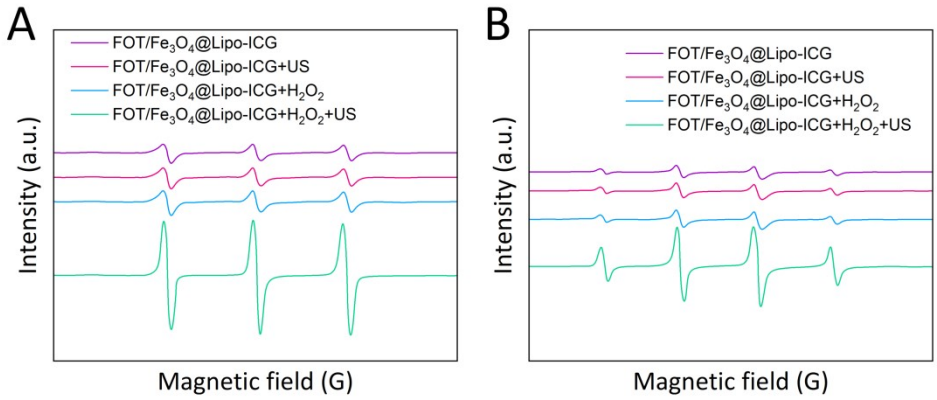

Figure S7. Electron spin resonance spectra of $^1O_2$ (A) and ·OH (B) in FOT/Fe_3O_4@Lipo-ICG and FOT/Fe_3O_4@Lipo-ICG+H_2O_2 dispersions after US irradiation or not. The concentration of H_2O_2 was 1 mM. US irradiation: 1.0 MHz, 1.0 W/cm^2, 40% cycle.

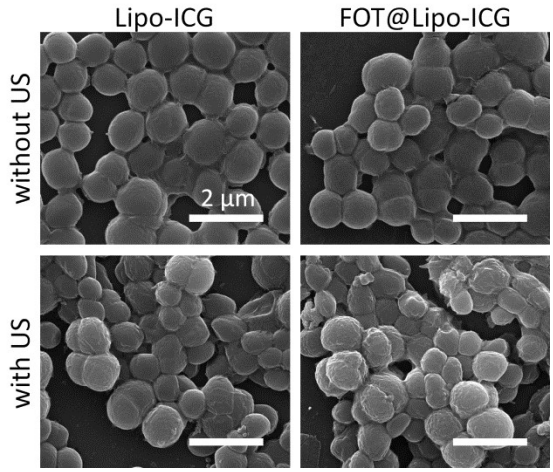

Figure S8. SEM images of MRSA after different treatments. US irradiation: 1.0 MHz, 1.0 W/cm^2, 40% cycle.

Figure S9. Photographs of the MRSA-infected skin during treatment with FOT/Fe_3O_4@Lip-ICG without US irradiation at 0, 6 and 12 days.

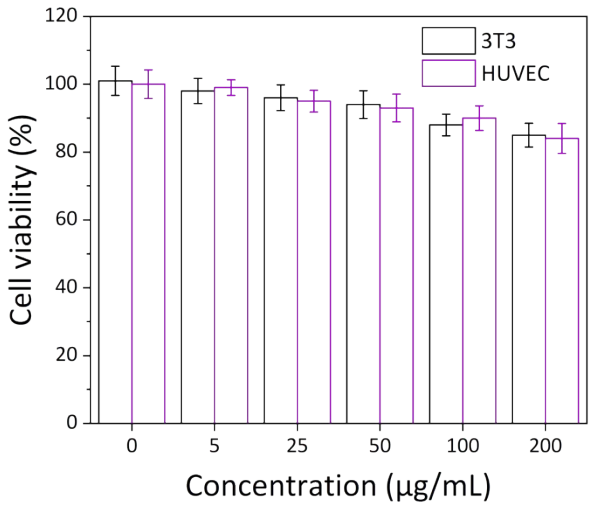

Figure S10. Cell viability of HUVEC and 3T3 treated with different concentrations of FOT/Fe_3O_4@Lipo-ICG. Data are presented as mean ± s.d. (n = 3).

Table S1. Properties of liposomes.

Entry	Liposomes	Size (nm)	PDI[a]	Zeta potential (mv)
1	Lipo-ICG	90.3 ± 7.4	0.18 ± 0.04	−22.5 ± 0.4
2	FOT@Lipo-ICG	140.2 ± 6.9	0.17 ± 0.02	−26.6 ± 0.2
3	FOT/Fe_3O_4@Lipo-ICG	165.1 ± 10.8	0.18 ± 0.02	−27.7 ± 0.5

[a] Polydispersity index (PDI).

Table S2. LE and EE of FOT/Fe_3O_4@Lipo-ICG.

Liposomes	LE[a] (%)		EE[b] (%)	
	FOT	Fe_3O_4	FOT	Fe_3O_4
FOT@Lipo-ICG	5.4 ± 0.6	–	70.0 ± 4.4	–
FOT/Fe_3O_4@Lipo-ICG	5.4 ± 0.5	8.0 ± 0.7	70.0 ± 3.2	80.0 ± 4.3

[a] Loading efficiency (LE).

[b]Entrapment efficiency (EE).